PHYSICAL REVIEW B **94**, 220401(R) (2016)

Vortex-dynamics-mediated low-field magnetization switching in an exchange-coupled system

Weinan Zhou,[1] Takeshi Seki,[1,2,*] Hiroko Arai,[2,3] Hiroshi Imamura,[3] and Koki Takanashi[1]
[1]*Institute for Materials Research, Tohoku University, Sendai 980-8577, Japan*
[2]*JST PRESTO, Saitama 332-0012, Japan*
[3]*National Institute of Advanced Industrial Science and Technology, Tsukuba 305-8568, Japan*
(Received 1 March 2016; revised manuscript received 20 August 2016; published 8 December 2016)

An aspect of a magnetic vortex whose dynamics strongly affects the magnetic structures of the environment is experimentally shown. We exploit a nanodot of an exchange-coupled bilayer with a soft magnetic $Ni_{81}Fe_{19}$ [permalloy (Py)] having a magnetic vortex and a perpendicularly magnetized $L1_0$-FePt exhibiting a large switching field (H_{sw}). The vortex dynamics with azimuthal spin waves makes the excess energy accumulate in the Py, which triggers reversed-domain nucleation in $L1_0$-FePt at a low magnetic field. Our experimental and numerical results shed light on the essence of reversed-domain nucleation, and provide a route for efficient H_{sw} reduction.

DOI: 10.1103/PhysRevB.94.220401

A magnetic vortex in a soft magnetic disk, a topological defect, is an in-plane curling magnetic structure having a core whose magnetic moments are normal to the disk plane [1,2]. Magnetic vortices have fascinated us because of their unique functionalities [3] and rich physics [4]. Several kinds of nonequilibrium dynamical motions can be excited by applying an rf magnetic field (H_{rf}) [4–6] or injecting spin current [7–9], leading to promising applications such as a vortex-type magnetic random access memory and a spin torque vortex oscillator. At certain conditions, the vortex polarity (core magnetization direction) and/or the circulation of in-plane magnetic moments can be switched [10–13]. Those studies focus on the control of magnetic moments in the vortex. Although the interplay of the vortex in a magnet and the magnetization in an adjacent exchange-coupled magnet was investigated in a previous paper [14], using magnetic vortex dynamics in a soft magnet as a route to switching the magnetization of a hard magnet has yet to be tried. Here, we show H_{rf}-induced vortex dynamics in soft magnetic permalloy (Py) triggers the magnetization switching of hard magnetic $L1_0$-FePt, which can balance the competing goals for reducing H_{sw} and maintaining the thermal stability of magnetization in a nanosized magnet.

We used the exchange-coupled system consisting of nanodots with a hard magnetic $L1_0$-FePt layer and a soft magnetic Py layer [Figs. 1(a) and 1(b)]. The thin films were grown on an MgO (100) single crystal substrate with a stack of MgO substrate‖Fe (1)|Au (60)|FePt (10)|Py (150)|Au (5)|Pt (3) (in nanometers). The $L1_0$-FePt (001) layer was epitaxially grown at 550°C on the Au (100) buffer layer. The thin film preparation is described in the Supplemental Material [15]. The thin films were microfabricated into circular nanodots with a diameter of 260 nm through the use of electron beam lithography and Ar ion milling. The 10-nm-thick $L1_0$-FePt had a large uniaxial magnetocrystalline anisotropy (K_u) along the perpendicular direction to the disk plane (z direction), whereas the 150-nm-thick Py possessed negligible magnetocrystalline anisotropy, but the nanodot shape induced the shape magnetic anisotropy. This enabled us to saturate the magnetic moments of Py in the z direction by applying a dc magnetic field (H) perpendicular to the disk plane that was lower than the demagnetizing field for the thin film form [16].

First, we performed micromagnetic simulations to reveal the equilibrium magnetic state. The mumax[3] package [17] was used for full micromagnetic simulations of the FePt|Py magnetic layers. The simulated structure was a cylindrical dot 200 nm in diameter and 10 nm (150 nm) in thickness for the FePt (Py) layer. The sample was divided into discrete computational cells, and the size of each cell was $3.125 \times 3.125 \times 2.5\,nm^3$. The saturation magnetization (M_s) and K_u for FePt were $1.15 \times 10^6\,A/m$ and $3.2 \times 10^6\,J/m^3$, respectively. The easy axis of the FePt was in the z direction. M_s and K_u for Py were $0.8 \times 10^6 A/m$ and $0 J/m^3$, respectively. We chose a stiffness constant of $A = 1.3 \times 10^{-11} J/m$ for the whole system. In this calculation, the damping parameter of $\alpha = 0.5$ was used for both materials in order to expedite relaxation to the equilibrium orientation. The simulated magnetization (M)-H curve is shown in Fig. 1(c), where M was normalized by the saturation value and H was applied along the z direction. The M-H curve exhibits a two-step behavior. As H is swept from $-10\,kOe$, M starts to increase at $H \sim -2.5\,kOe$. As depicted in Fig. 1(d), at $H = 0\,kOe$, the magnetic vortex is formed in Py whereas all the magnetic moments in $L1_0$-FePt saturate along the $-z$ direction. The vortex structure has a small deformation, in which the magnetic moments are slightly tilted from the azimuthal direction of the disk to the radial direction. As H increases to 2.6 kOe, the magnetic moments are tilted to the $+z$ direction [m_z in Fig. 1(e)], although the vortex structure is still maintained [m_x in Fig. 1(e)]. Increasing H to 5 kOe compresses the vortex structure in Py to the interface, in which the core polarity is switched [Fig. 1(f)]. By comparing the cross-sectional x-y images near the interface [Figs. 1(e) and 1(f)], one can see that there is no remarkable change in the m_x component even for the compressed vortex structure. These magnetic states are totally different from the spatially twisted magnetic structures observed in the in-plane magnetized $L1_0$-FePt|Py bilayers [18].

Next, we experimentally examined the question of whether the vortex dynamics in Py affects H_{sw} in $L1_0$-FePt. The magnetization curves for the dot arrays were measured using a superconducting quantum interference device magnetometer

*Corresponding author: go-sai@imr.tohoku.ac.jp

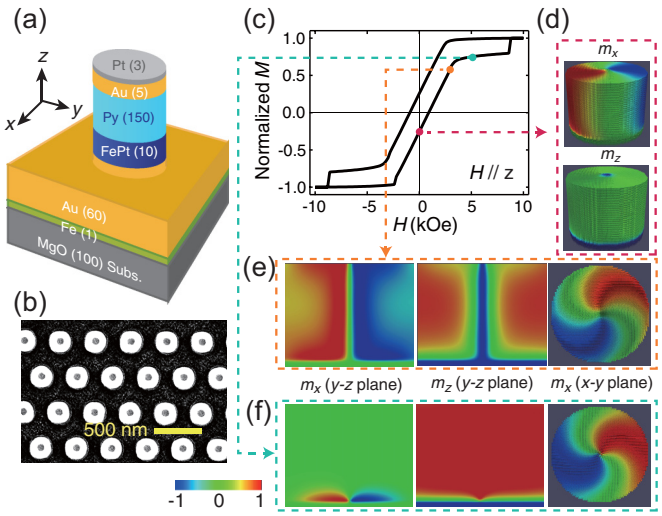

FIG. 1. (a) Schematic illustration of a microfabricated dot of a $L1_0$-FePt |permalloy (Py) exchange-coupled system. (b) Scanning electron microscope image for the array of dots. (c) Simulated magnetization (M) vs the dc magnetic field (H), where M was normalized by the saturation value and H was applied along the z direction. (d) Simulated structures of magnetic moments (m) of the x component (m_x, upper panel) and the z component (m_z, lower panel) at $H = 0$ Oe. (e) and (f) Simulated magnetic structures of m_x in the y-z plane (left panel), m_z in the y-z plane (middle panel), and m_x in the x-y plane (right panel) at $H = 2.6$ and 5 kOe.

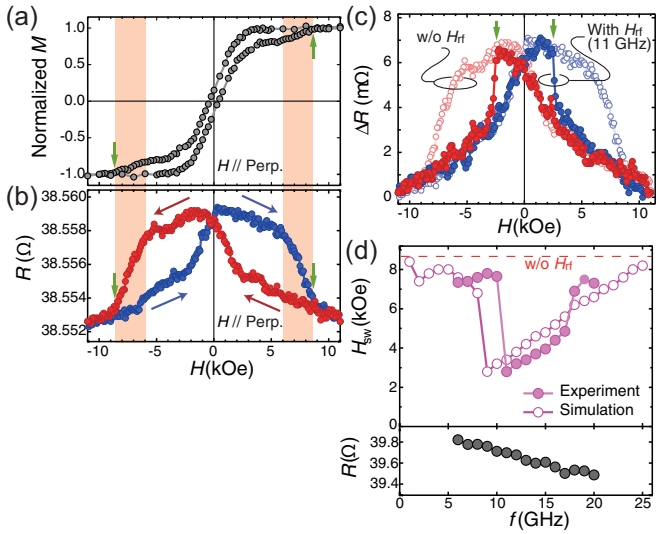

FIG. 2. (a) M as a function of H for microfabricated dots with $L1_0$-FePt|Py, where the value of M was normalized by the saturation magnetization. (b) Device resistance (R) as a function of H without the rf magnetic field (H_{rf}). (c) ΔR-H curves with H_{rf} (solid circles) and without H_{rf} being applied (open circles). ΔR is the resistance change from R at $H = -11$ kOe. 22 dBm of rf power was applied to the device, which corresponded to $H_{rf} = 200$ Oe. The frequency (f) of H_{rf} was set at 11 GHz. For both M-H and R-H curves, H was applied perpendicularly to the device plane. The thick arrows denote the switching fields (H_{sw}) of $L1_0$-FePt. (d) H_{sw} (top panel) and R at $H = -11$ kOe (bottom panel) as a function of f. The dotted line denotes H_{sw} without H_{rf}, and the solid (open) circles represent the experimental (simulated) results.

at room temperature. Figure 2(a) displays the full M-H curve exhibiting a two-step magnetization reversal behavior similar to the simulation. When H was swept from positive to negative, the magnetization switching of the $L1_0$-FePt occurred in the range from -6 to -9 kOe. The minor magnetization curves showing springback behavior, which are given in the Supplemental Material [15], also suggest that the magnetic moments of $L1_0$-FePt (m^{FePt}) were switched in the hatched H region in Fig. 2(a). It is noted that both the perpendicular and in-plane magnetization curves showed low remanent magnetization, which resulted from the formation of a magnetic vortex in Py (see Fig. S3 in the Supplemental Material [15]).

In order to evaluate H_{sw} of $L1_0$-FePt under vortex dynamics excitation in Py, we measured the anisotropic magnetoresistance (AMR) effect for the nanodot array located on a coplanar waveguide (CPW) using a lock-in amplifier (see the Supplemental Material for the measurement setup [15]). The Au buffer layer was patterned into the CPW with a signal line of 4 μm $\times$ 50 μm, and an array of more than 1000 dots of the FePt|Py bilayer was placed on the signal line. Figure 2(b) shows the electrical resistance (R) as a function of H without H_{rf} being applied. At large positive H, e.g., $H = 9$ kOe, all the magnetic moments in the bilayer were aligned with H, giving a low R value. As H decreased, m^{FePt} maintained a positive value while the magnetic moments in Py(m^{Py}) rotated gradually, forming a spatially nonuniform magnetic structure. The part of m^{Py} directed along the signal line of the CPW increased the value of R due to the AMR effect. As H decreased further, m^{FePt} started to switch and eventually all the magnetic moments saturated again at $H = -9$ kOe. As indicated by the hatched areas in Figs. 2(a) and 2(b), the H regions showing the switching of m^{FePt} in the R-H curve are in good agreement with those in the full M-H curve. In the case of no H_{rf}, i.e., no excitation of vortex dynamics, H_{sw} is found to be 8.6 kOe, as indicated by the green arrows.

To excite the vortex dynamics in Py, we applied H_{rf} transverse to the signal line of the CPW by injecting an rf power of 22 dBm from a signal generator, which corresponded to $H_{rf} = 200$ Oe. The representative ΔR-H curve is shown in Fig. 2(c), where ΔR is the resistance change from R at $H = -11$ kOe. The frequency (f) of H_{rf} was 11 GHz. The shape of the $\Delta R - H$ curve for $f = 11$ GHz (solid circles) is rather different from that without H_{rf} (open circles). R sharply drops to the low R state at $H = \pm 2.8$ kOe, indicating that applying H_{rf} with $f = 11$ GHz significantly reduces H_{sw}. Figure 2(d) summarizes H_{sw} and R as a function of f. Compared to the value of H_{sw} with no H_{rf} applied, one can see a small decrease in H_{sw} in the whole f region when 22 dBm of rf power was injected. This f-independent decrease is attributable to Joule heating caused by high rf power injection. In addition to the f-independent decrease, a strong reduction of H_{sw} is evident in the range of $11 \leqslant f \leqslant 17$ GHz. In this f range, H_{sw} gradually increases, and the values of H_{sw} in $f \geqslant 18$ GHz are almost the same as those in $6\,\mathrm{GHz} \leqslant f \leqslant 10\,\mathrm{GHz}$. This reduction is not due to Joule heating because R reflecting the device temperature does not show any correlation with H_{sw}. We can also exclude the possibility that the excitation of uniform

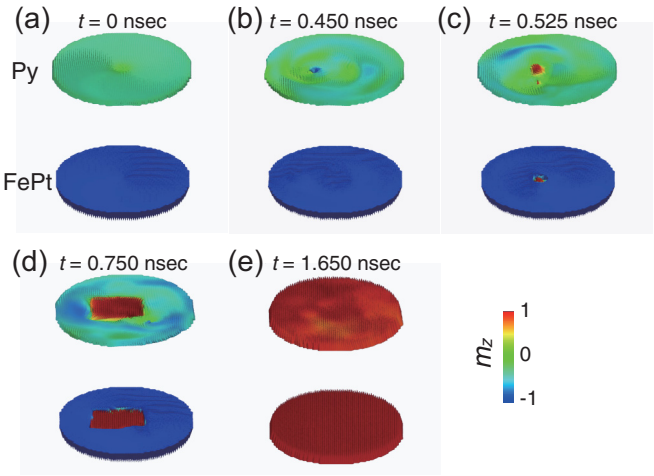

FIG. 3. (a)–(e) Snapshots for m_z at $H = 3.4$ kOe under an application of H_{rf} with $f = 11$ GHz. The top and bottom panels are x-y plane images for Py and FePt, respectively. The planes of the Py and FePt slices are 2 and 5 nm, respectively, away from the FePt|Py interface.

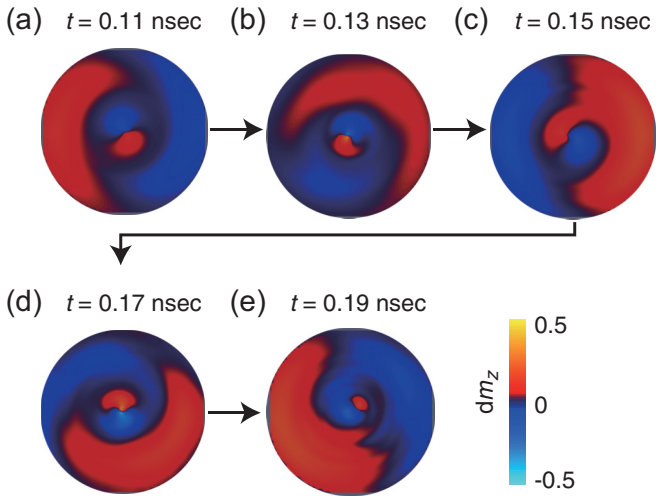

FIG. 4. (a)–(e) Snapshots for deviation of $m_z(dm_z)$ for Py at $H = 3.4$ kOe under the application of H_{rf} with $f = 11$ GHz. The plane of the Py slice was 2 nm away from the FePt|Py interface.

magnetization dynamics in $L1_0$-FePt could lead to low H_{sw} because the resonance frequency of $L1_0$-FePt is estimated to be about 170 GHz. The magnetization dynamics under H_{rf} was calculated by applying $H_{ext}(t) = [0, H' \sin(2\pi f t), H]$, where H' and f are the amplitude and frequency of H_{rf}, respectively. The amplitude H' was set to be 200 Oe. For the magnetization dynamics calculation, the values of α were set at 0.1 for FePt and 0.01 for Py. Thermal effects were neglected throughout the simulation for simplicity. The numerical simulation reproduces the experimental results of f dependence of H_{sw}, as shown by the open circles in Fig. 2(d).

Figures 3(a)–3(e) show snapshots of the time evolution of m_z for $f = 11$ GHz and $H = 3.4$ kOe [19]. The sliced planes of Py (top panels) and FePt (bottom panels) are 2 and 5 nm, respectively, away from the $L1_0$-FePt|Py interface. The inhomogeneous dynamics is excited in the Py [Figs. 3(b)–3(d)]. At $t = 0.525$ ns, reversed-domain nucleation occurs in $L1_0$-FePt beneath the vortex core in Py [Fig. 3(c)]. The reversed domain expands coherently in Py and $L1_0$-FePt [Fig. 3(d)]. A similar inhomogeneous dynamics is excited for all conditions of f when H_{sw} is reduced (see Fig. S5 in the Supplemental Material [15]). Now let us discuss the magnetization switching process induced by vortex dynamics. Several excitations such as the gyrotropic motion of the vortex core, azimuthal spin waves, and radial spin waves have been observed in H_{rf}-induced vortex dynamics for a single soft magnetic disk [6,20–22]. In order to assign which dynamical mode is responsible for the switching we observed, we calculated the deviation of the magnetization (dm) from the equilibrium state. The time evolutions of the z-component dm (dm_z) at $f = 11$ GHz are displayed in Fig. 4. The borders between the red region (positive dm_z) and blue one (negative dm_z) correspond to the nodes of spin waves. One sees that there are several nodes exhibiting clockwise rotation, in which the wave vectors of spin waves are along the azimuthal direction. In addition, we have the node surrounding the vortex core. This node is attributable to the standing spin wave along the radial direction. Consequently, we consider that the eigenmode is the azimuthal spin wave having a node in the radial direction. Although these analyses are performed based on simulated results, the experimental ferromagnetic resonance spectra are in agreement with the simulated spectra (see Fig. S6 in the Supplemental Material [15]). Thus, the above eigenmodes have also been confirmed experimentally. Although we also phenomenologically analyzed our data based on the macrospin model, described in the Supplemental Material [15], the phenomenological analysis did not properly reproduce our results, supporting nonuniform magnetization reversal in the present system.

In Fig. 4, near the vortex core located at the center, dm_z shows a steep spatial change in the narrow region. The azimuthal rotation of the spin wave enlarges the area of the vortex core or produces multiple vortex cores in some cases. When the area of the vortex core reaches a critical size, reversed-domain nucleation occurs in $L1_0$-FePt. We quantitatively evaluate the nucleation volume in $L1_0$-FePt from the measurement temperature (T) dependence of H_{sw} without H_{rf} [Fig. 5(a)]. According to the Néel-Arrhenius law, the T dependence of H_{sw} can be fitted by [23]

$$H_{sw}(T) = H_{sw,0}(T)\left\{1 - \sqrt{\frac{k_B T}{E_0(T)} \ln\left(\frac{k_B T}{E_0(T)} H_{sw,0}(T) \frac{f_0}{R}\right)}\right\}, \quad (1)$$

where $H_{sw,0}$ is the switching field without thermal agitation, k_B is the Boltzmann constant, and E_0 is the energy barrier given by the product of K_u and the magnetic volume (V). f_0 is the attempt frequency (10^9Hz). R is the rate of H sweep (10 Oe/s). We assume no remarkable T dependence of $H_{sw,0}$ as previously reported for FePt [24]. $H_{sw,0}$ and E_0 are found to be 14.4 ± 0.7 kOe and $(0.9 \pm 0.3) \times 10^{-18}$J, respectively. Using $K_u = 3.1 \times 10^6$ J/m^3 evaluated experimentally from the M-H curves for the FePt single layer, we obtain $V = 300 \pm 100$ nm^3, which corresponds to the nucleation volume under the static H ($V^{nuc,H}$). On the other hand, the nucleation

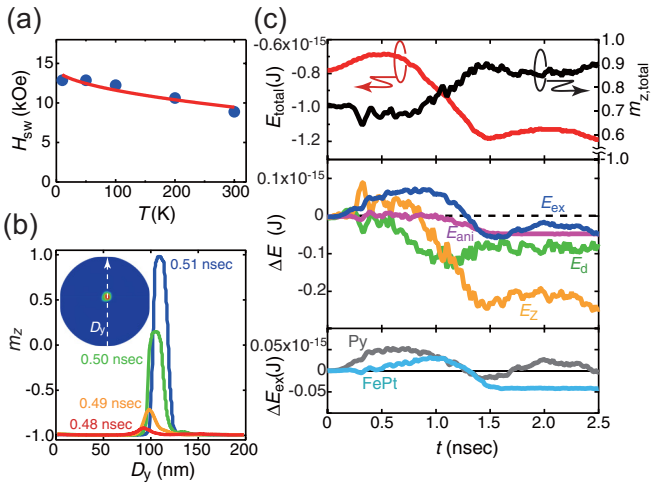

FIG. 5. (a) H_{sw} as a function of measurement temperature (T) experimentally obtained without H_{rf}. The solid line denotes the result of fitting. (b) m_z at $H = 3.4$ kOe as a function of the position in the dot along the in-plane y direction (D_y) at various times (t). D_y is denoted in the inset. The plane of the FePt slice was 5 nm away from the FePt|Py interface. (c) Top panel: Calculated t dependence of total $m_z(m_{z,total})$ and total energy (E_{total}). Since H was set at 3.4 kOe, $m_{z,total}$ shows a value of ~0.7 before the reversed-domain nucleation. Middle panel: t-dependent energy difference (ΔE) for Zeeman energy (E_Z), demagnetizing energy (E_d), exchange energy (E_{ex}), and anisotropy energy (E_{ani}). Bottom panel: t dependence of ΔE_{ex} in Py and $L1_0$-FePt.

volume under the excitation of vortex dynamics ($V^{nuc,D}$) is estimated numerically. Let us once again look at the case of FePt switching under H_{rf} of $f = 11$ GHz and $H = 3.4$ kOe. Figure 5(b) displays simulated m_z as a function of the position in the dot along the in-plane y direction (D_y) at various t. At $t = 0.51$ ns, the region having $m_z > 0.9$ appears, which is defined as $V^{nuc,D}$. Thus $V^{nuc,D}$ is estimated to be $\sim 800\,\mathrm{nm}^3$. This $V^{nuc,D}$ is comparable to $V^{nuc,H}$, suggesting that both nucleation processes have comparable E_0. We calculated the t dependence of total $m_z(m_{z,total})$ and total energy (E_{total}), which is the sum of Zeeman energy (E_Z), demagnetizing energy (E_d), exchange energy (E_{ex}), and anisotropy energy (E_{ani}) [Fig. 5(c)]. E_{total} gradually increases just after starting the vortex dynamics excitation, and then E_{total} decreases whereas m_z increases. As shown in the middle panel of Fig. 5(c), the time-dependent energy difference (ΔE) indicates that only E_{ex} contributes to the increase of E_{total}. At $t = 0.51$ ns, the excess $\Delta E_{ex} = 5 \times 10^{-17}$J is accumulated mainly in Py [bottom panel of Fig. 5(c)], which is large enough to overcome $E_0 = (0.9 \pm 0.3) \times 10^{-18}$J. This value of ΔE_{ex} in Py is comparable to the increase in ΔE_{ex} of 3×10^{-17}J in FePt resulting from the emergence of the domain wall. In other words, the main physical mechanism is that the ΔE_{ex} in Py acts as a driving force for overcoming the energy required for a reversed-domain expansion in $L1_0$-FePt. This is regarded as a nonlocal phenomenon in a coupled system. Again, we emphasize that mere vortex core switching does not nucleate the reversed domain in $L1_0$-FePt [Fig. 1(c)] and vortex dynamics excitation is essential for reversed-domain nucleation. Our results lead not only to insight into the nucleation phenomena but also a way for information writing of magnetic storage and spintronic applications using topological defects.

This work was partially supported by a Grant-in-Aid for Young Scientists A (25709056) and Grant-in-Aid for Scientific Research S (23226001). The device fabrication was partly performed at the Cooperative Research and Development Center for Advanced Materials, IMR, Tohoku University.

[1] R. P. Cowburn, D. K. Koltsov, A. O. Adeyeye, M. E. Welland, and D. M. Tricker, Phys. Rev. Lett. **83**, 1042 (1999).

[2] T. Shinjo, T. Okuno, R. Hassdorf, K. Shigeto, and T. Ono, Science **289**, 930 (2000).

[3] S. Bohlens, B. Krüger, A. Drews, M. Bolte, G. Meier, and D. Pfannkuche, Appl. Phys. Lett. **93**, 142508 (2008).

[4] S.-B. Choe, Y. Acremann, A. Scholl, A. Bauer, A. Doran, J. Stöhr, and H. A. Padmore, Science **304**, 420 (2004).

[5] M. Buess, R. Höllinger, T. Haug, K. Perzlmaier, U. Krey, D. Pescia, M. R. Scheinfein, D. Weiss, and C. H. Back, Phys. Rev. Lett. **93**, 077207 (2004).

[6] V. Novosad, F. Y. Fradin, P. E. Roy, K. S. Buchanan, K. Y. Guslienko, and S. D. Bader, Phys. Rev. B **72**, 024455 (2005).

[7] S. Kasai, Y. Nakatani, K. Kobayashi, H. Kohno, and T. Ono, Phys. Rev. Lett. **97**, 107204 (2006).

[8] V. S. Pribiag, I. N. Krivorotov, G. D. Fuchs, P. M. Braganca, O. Ozatay, J. C. Sankey, D. C. Ralph, and R. A. Buhrman, Nat. Phys. **3**, 498 (2007).

[9] A. Dussaux, B. Georges, J. Grollier, V. Cros, A. V. Khvalkovskiy, A. Fukushima, M. Konoto, H. Kubota, K. Yakushiji, S. Yuasa, K. A. Zvezdin, K. Ando, and A. Fert, Nat. Commun. **1**, 8 (2010).

[10] B. Van Waeyenberge, A. Puzic, H. Stoll, K. W. Chou, T. Tyliszczak, R. Hertel, M. Fähnle, H. Brückl, K. Rott, G. Reiss, I. Neudecker, D. Weiss, C. H. Back, and G. Schütz, Nature (London) **444**, 461 (2006).

[11] M. Kammerer, M. Weigand, M. Curcic, M. Noske, M. Sproll, A. Vansteenkiste, B. Van Waeyenberge, H. Stoll, G. Woltersdorf, C. H. Back, and G. Schütz, Nat. Commun. **2**, 279 (2011).

[12] K. Yamada, S. Kasai, Y. Nakatani, K. Kobayashi, H. Kohno, A. Thiaville, and T. Ono, Nat. Mater. **6**, 269 (2007).

[13] V. Uhlíř, M. Urbánek, L. Hladík, J. Spousta, M.-Y. Im, P. Fischer, N. Eibagi, J. J. Kan, E. E. Fullerton, and T. Šikola, Nat. Nanotechnol. **8**, 341 (2013).

[14] P. Wohlhüter, M. T. Bryan, P. Warnicke, S. Gliga, S. E. Stevenson, G. Heldt, L. Saharan, A. K. Suszka, C. Moutafis, R. V. Chopdekar, J. Raabe, T. Thomson, G. Hrkac, and L. J. Heyderman, Nat. Commun. **6**, 7836 (2015).

[15] See Supplemental Material at http://link.aps.org/supplemental/10.1103/PhysRevB.94.220401 for the details of experimental procedure, the results of magnetization measurements and

dynamics measurements, and the calculated results from the micromagnetic simulation and the macrospin model.

[16] W. Zhou, T. Seki, H. Iwama, T. Shima, and K. Takanashi, J. Appl. Phys. **117**, 013905 (2015).

[17] A. Vansteenkiste, J. Leliaert, M. Dvornik, M. Helsen, F. Garcia-Sanchez, and B. Van Waeyenberge, AIP Adv. **4**, 107133 (2014).

[18] T. Seki, K. Utsumiya, Y. Nozaki, H. Imamura, and K. Takanashi, Nat. Commun. **4**, 1726 (2013).

[19] See Supplemental Material at http://link.aps.org/supplemental/10.1103/PhysRevB.94.220401 for a movie showing the time evolution of m_z components in Py and $L1_0$-FePt.

[20] I. Neudecker, K. Perzlmaier, F. Hoffmann, G. Woltersdorf, M. Buess, D. Weiss, and C. H. Back, Phys. Rev. B **73**, 134426 (2006).

[21] F. G. Aliev, J. F. Sierra, A. A. Awad, G. N. Kakazei, D.-S. Han, S.-K. Kim, V. Metlushko, B. Ilic, and K. Y. Guslienko, Phys. Rev. B **79**, 174433 (2009).

[22] X. Zhu, Z. Liu, V. Metlushko, P. Grütter, and M. R. Freeman, Phys. Rev. B **71**, 180408(R) (2005).

[23] M. El-Hilo, A. M. de Witte, K. O'Grady, and R. W. Chantrell, J. Magn. Magn. Mater. **117**, L307 (1992).

[24] N. Kikuchi, S. Okamoto, O. Kitakami, Y. Shimada, and K. Fukamichi, Appl. Phys. Lett. **82**, 4313 (2003).